

Emissions-Based Environmental Impact Analysis from a Power-Cooling Organic Rankine Cycle with Ejector System

¹Ukemeobong E. Akpan, ²Bassey D. Nkanang, ³Agnes E. Oboh,
⁴Oyongha M. Agbiji, ⁵Remigus A. Umunnah, ⁶Obasi-sam O. Ojobe,
⁷Patrick O. Odu.

¹Department of Mechanical Engineering, Topfaith University, Mkpatak, Akwa Ibom State, Nigeria

²Department of Mechanical Engineering, Akwa Ibom State University, Ikot Akpaden, Nigeria

³Department of Mechanical Engineering, University of Uyo, Akwa Ibom State, Nigeria

^{4&5}Department of Mechanical Engineering, University of Calabar, Calabar, Nigeria

^{6&7}Department of Electrical & Electronics Engineering, University of Calabar, Calabar, Nigeria

Abstract

Although Organic Rankine cycles does not require the combustion of its working fluid, the choice of operating refrigerants pose significant environmental impact from construction, operation and decommissioning phases. This research work focused on the evaluation of possible environmental impacts of an adapted power-cooling organic Rankine cycle using six different refrigerants with respect to the power generation potential within the system's operational phase. A simplified life cycle model was used for quantifying the related emissions subject to the thermodynamic operation of the cycle for each refrigerant. The analysis was done using the Engineering Equation Solver. The results revealed R114 and R600a as the refrigerants with the highest emissions of greenhouse gases amongst all others when all refrigerants are operating under the same conditions, but with the potential to generate the highest power from the system. Within the estimated 20 years system life cycle, the system can emit as much as 6.5 tons of carbon dioxide equivalent, while generating 66 KW of turbine power with R113 as the working fluid. The results can assist in the optimal refrigerant choice with regards to environmental sustainability, operating cost, and performance efficiency in the adapted power-cooling system.

Keywords: Environmental impact, organic Rankine cycle, power-cooling, refrigerants, thermodynamic operation, environmental sustainability.

1. Introduction

The organic Rankine cycle (ORC) is recognized as a highly developed means for harnessing the waste heat from industrial processes and other low-temperature heat sources in the conversion of thermal power to electrical energy (Mondejar et al., 2018). It offers the flexibility of a bottoming cycle to various low-grade energy sources for additional power generation, and also other products like refrigeration and district water heating (Yu et al., 2013; Guzović et al., 2014; Ayub et al., 2015). The ORC derives its driving energy via a heat exchange between an evaporator and the low-grade heat flare gas. Although the ORC system does not require the combustion of its working fluid during operation, organic refrigerants used as its working fluid are susceptible to non-direct emissions of greenhouse gasses (GHGs) including carbon dioxide during either the production, operation and decommissioning phases. Therefore, the choice of eco-friendly refrigerants is a necessity during the design process.

ORC refrigerants, based on their classification, possess negative environmental impacts linked to their global warming potential (GWP) and human toxicity potential (HTP). Amongst some considered environmental impacts, the most serious one is the GWP, followed by the HTP (Liu et al., 2013). In reference to the GWP of refrigerants, GHGs dominate as a cause of global warming, including residual heat and waste heat (Bian, 2020). As for HTP, the major pollutants that give rise to it are CO, NO_x, and SO_x (Li et al., 2012). There is therefore a need for the evolution of these gases and by-products (residual/waste heat) of industrial processes to be minimized or utilized respectively.

This can be done by performing a greenhouse gas emissions evaluation to ascertain gases (and in what quantity) are released by various organic working fluids in ORCs especially with respect to leakages.

Furthermore, the GHG emissions evaluation in ORCs assists in identifying the impact they have on the environment and to make a decision to utilize the most effective and safest options. Research and development can even lead to the synthesis of new working fluids that meet the acceptable standards. Studies on the environmental impact of ORCs and their working fluid are already in the public domain, but relatively few (Park et al., 2019; Liu et al., 2013). For example, Liu et al., (2013) evaluated the environmental impact of an organic Rankine cycle power-plant for waste-heat-recovery using life cycle analysis methodology during the construction, operation and decommissioning phases of the plant. They listed the inventory of environmental emissions for the plant using 7 different working fluids. Wang et al., (2019) evaluated a carbon footprint for an ORC using zeotropic mixture and concluded that the primary source of CO₂ emissions emanates from ORC heat exchangers and also during leak process. Further studies also indicate indirect methods for reduction of emissions in ORC by optimization of component performance. Thus, Mohammadzadeh et al., (2017) showed that installing an internal heat exchanger in an ORC system can bring about 3.6 % reduction in carbon dioxide emissions than conventional ORC. Due to the potential for environmental impact from ORC systems, the quantification of these emissions is pertinent, based on the structure and size of the operating cycle, as well as the working refrigerants, especially throughout the system life cycle. Accordingly, the research is focused on the evaluation of possible environmental impacts of an adapted power-cooling organic Rankine cycle using six different refrigerants with respect to the power generation potential within the system's operational phase. A simplified life cycle model was used for quantifying the related emissions subject to the thermodynamic operation of the cycle for each refrigerant.

2.0 Objectives

- To evaluate the possible environmental impacts of an adapted power-cooling organic Rankine cycle using six different refrigerants with respect to the power generation potential within the system's operational phase.
- To assess the parameter on which the emissions produced in the turbine depend.

3.0 Methodology

3.1 Materials

The adapted ORC for cooling and power generation is shown in Fig. 1. The system is made up of various components including a vapour generator, an expander (or turbine), an ejector, a pump, throttling valve, evaporator, and a condenser.

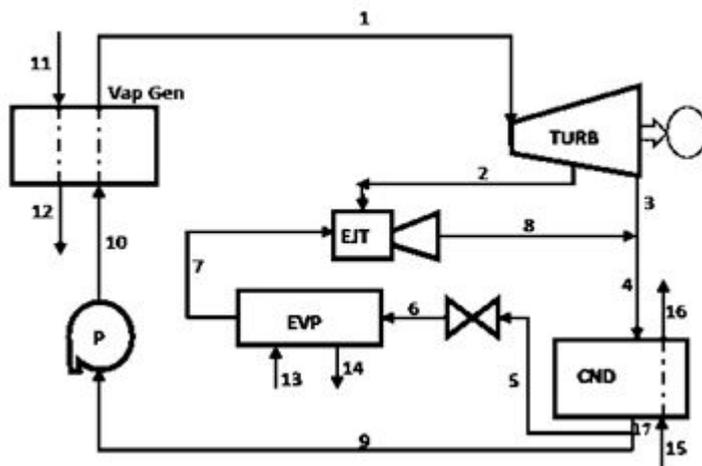


Figure 1: Schematic Diagram of the ORC for power and cooling (Abam et al., 2022)

The series of steps through which the system performs its functions are described as follows: Power is provided to the system by low-grade waste heat from any industrial process providing low grade heat. The heat is used to increase the energy level of the circulating refrigerants via a heat exchanger herein referred to a vapour generator. The refrigerant gets vaporized to a super-heated vapour at state 1 before it is directed and passed through a turbine to expand, thus, producing work and driving a generator to produce power. However, before the vaporized refrigerant is fully expanded, it is bled out of the turbine at state 2 to pass through the ejector nozzle. Upon exiting the ejector nozzle, the vaporized refrigerant has a high velocity, and this spurs the creation of a vacuum at the entrance into the mixing chamber. The created vacuum in the ejector mixing chamber at state 2 causes an inflow of secondary vapour (state 7) out of the evaporator to the mixing chamber and the exit stream (state 8) gets mixed with the expanded refrigerant vapour coming out of the turbine (state 3) at state 4. The mixture at state 4 passes to the condenser, inside which it gets water-cooled and condenses to a saturated liquid. On exiting the condenser at state 17, the liquid refrigerant gets split along two routes (states 5 and 9). The route through state 5 takes it into an expansion/throttling valve to reduce both its temperature and pressure so it can be evaporated to produce cooling in the evaporator at state 6. The evaporation happens because the refrigerant absorbs the heat from the substance placed in the evaporator; this is how the cooling effect is made on the substance. The second path out of the condenser through state 9 leads the saturated liquid to a pump where it is pressurized and sent to the vapour generator to start the cycle again. The working fluids (refrigerants) used in the operation of the ORC power/cooling system are R113, R114, R123, R141b, R245fa, and R600a. The operating thermodynamic assumptions adopted for the analysis are summarised as follows (Abam et al., 2022):

In all components, there is a steady flow condition for the refrigerant. Losses due to friction, heat, and pressure in the components are negligible. Adiabatic system boundaries, thus, heat loss to the environment is negligible. Heat is provided from a modular turbine's exhaust gas estimated at 623 K, and the mass flux for the heat source was taken as 20 kg/s. The isentropic efficiencies of the pump and turbine are 70 % and 85 %, respectively. The pinch point temperature difference for the evaporator is kept at 278 K while that of the condenser is kept at 283 K. The ambient temperature was referenced at 293.17 K. The efficiencies of the nozzle, diffuser, and mixer unit in the ejector are 85 %, 85 %, and 95 %, respectively. There is an isobaric mixture process inside of the ejector mixing chamber. The nozzle exit pressure equals the inlet secondary pressure (Abam et al., 2022; Manente et al., 2017)

3.2 Methods

3.2.1 Thermodynamic modelling

The system's operating parameters were evaluated at component level based on the first law of thermodynamics. Using the steady flow energy equation, and neglecting all potential and kinetic energy interaction in the system, the general energy balance for the k^{th} component is expressed as (Bronicki, 2017; Cao et al., 2017):

$$\sum \dot{W}_k - \sum \dot{Q}_k = \sum_{i,e}^{m,n} |\dot{m}_i \dot{h}_i - \dot{m}_e \dot{h}_e| \quad 1$$

Where, the work and heat requirements in the k^{th} component are denoted with \dot{W}_k and \dot{Q}_k , respectively, while the mass and enthalpy are represented with m and h . The subscripts, i and e , are for flow inlet and outlet, respectively. The energy balance for the components is shown in Table 1.

Table 1: Process energy balance for each component

Component	Energy balance
Vapor generator	$\dot{m}_{11}h_{11} + \dot{m}_{10}h_{10} = \dot{m}_1h_1 + \dot{m}_2h_2$
Turbine	$\dot{m}_1h_1 + W_{turb} = \dot{m}_2h_2 + (1-x)(h_2 - h_3) \times \eta_{isen, turb}$
Throttling valve	$\dot{m}_5h_5 = \dot{m}_6h_6$
Condenser	$\dot{m}_4h_4 - \dot{m}_{17}h_{17} = \dot{m}_{16}h_{16} - \dot{m}_{15}h_{15}$
Ejector	$\dot{m}_2h_2 + \dot{m}_7h_7 = \dot{m}_8h_8$
Pump	$\dot{W}_{pump} = \dot{m}_{10}(h_{10} - h_9) \times \eta_{isen, pump}$
Evaporator	$\dot{m}_6h_6 + \dot{m}_{13}h_{13} = \dot{m}_7h_7 + \dot{m}_{14}h_{14}$

3.2.1.1 Modelling of the ejector

The data used to model the ejector was acquired from (Haghparast et al., 2019; Mondal and De, 2017). With respect to the schematic of Fig. 1, the entrainment ratio for the secondary flow can be expressed as:

$$\omega = \frac{\dot{m}_7}{\dot{m}_2} \quad 2$$

The primary flow $V_{pf, n1}$ has a negligible inlet velocity at the nozzle. Thus, the primary flow outlet velocity, outlet enthalpy, and the efficiency of the nozzle, are denoted with the expressions (Haghparast et al., 2019).

$$V_{pf, n2} = \sqrt{2\eta_{Noz}(h_{pf, n1} - h_{pf, n2, s})} \quad 3$$

$$\eta_{Noz} = \frac{h_{pf, n1} - h_{pf, n2}}{h_{pf, n1} - h_{pf, n2, s}} \quad 4$$

Where: $h_{pf, n1}$ = enthalpy at point 7; $h_{pf, n2, s}$ = exit enthalpy of the primary flow under isentropic expansion; and η_{Noz} = nozzle efficiency. The mixing chamber area has an equation for the conservation of momentum that is given by:

$$\dot{m}_2V_{pf, n2} + \dot{m}_7V_{sf, n2} = (\dot{m}_2\dot{m}_7)V_{mf, m, s} \quad 5$$

In comparison with the primary flow velocity $V_{pf, n2}$, if the secondary flow velocity $V_{sf, n2}$ were neglected, then the outlet velocity of mixed flow $V_{mf, m,s}$ will be:

$$V_{mf, m,s} = \frac{V_{pf, n2}}{1+\omega} \quad 6$$

The mixing chamber efficiency is given as:

$$\eta_{Mix} = \frac{V_{mf,m}^2}{V_{mf,ms}^2} \quad 7$$

Thus, the velocity of the mixed flow can be given by:

$$V_{mf, m,s} = \frac{V_{pf, n2} \sqrt{\eta_{Mix}}}{V_{mf,ms}^2} \quad 8$$

The mixing chamber energy equation gives the equation:

$$\dot{m}_2 \left(h_{pf, n2} + \frac{V_{pf,n2}^2}{2} \right) + \dot{m}_7 \left(h_{sf, n2} + \frac{V_{sf,n2}^2}{2} \right) = \dot{m}_8 \left(h_{mf,m} + \frac{V_{mf,m}^2}{2} \right) \quad 9$$

Equations (8) and (9) are simplified to give the mixed flow enthalpy as:

$$h_{mf,m} = \frac{h_{pf, n1} + \omega h_{sf, n2}}{1+\omega} - \frac{V_{mf, m}^2}{2} \quad 10$$

At the diffuser of the ejector, the velocity of the mixed flow is converted to an increase in pressure. Taking the efficiency of the diffuser into account, and upon the assumption that the outlet velocity of the mixed fluid is negligible, the actual diffuser efficiency and outlet enthalpy of the mixed flow are expressed as:

$$h_8 = h_{mf,m} + \frac{(h_{mf,ds} - h_{mf,m})}{\eta_{Dif}} \quad 11$$

$$\eta_{Dif} = \frac{h_{mf, ds} - h_{mf, m}}{h_{mf, d} - h_{mf, m}} \quad 12$$

Where:

$h_{mf,ds}$ = ideal outlet enthalpy of the mixed flow with isentropic compression; and
 η_{Dif} = diffuser efficiency.

The entrainment ratio can be computed using Equation 13 (Haghparast et al., 2019).

$$\omega = \sqrt{\eta_{Noz} \eta_{Mix} \eta_{Dif} \left(\frac{h_2 - h_a}{h_3 - h_b} \right)} - 1 \quad 13$$

With the nozzle efficiency denoted with, nozzle mixing chamber efficiency, and diffuser efficiency, respectively represented with the terms η_{Noz} , η_{Mix} , and η_{Dif} in that order.

3.2.1.2 System environmental impact modeling

The environmental impact estimation is done using the relationship (Liu et al., 2013):

$$E_p(j) = \sum E_p(j)_i = \sum [Q(j)_i \cdot E_f(j)_i] \quad 14$$

In equation 14, the relative contribution of the j^{th} phase (capturing the construction, operation and decommissioning phases) to the environmental impact of the system is denoted with $E_p(j)$, while

the contribution of the i^{th} element of impact to the j^{th} phase is labelled as $E_p(j)_i$. Similarly, the size of emissions and the equivalent emissions factor from the i^{th} element are represented as $Q(j)_i$ and $E_f(j)_i$, respectively. The environmental impacts were computed only for the operational phase of the plant using R113, R114, R123, R141b, R245fa, and R600a refrigerants.

4.0 Results and discussion

The simulation results were performed using the Engineering Equation Solver (EES) based on component energy balance and the initial operating data in section 2.0. A detailed quantification of the operating system properties with R113, R114, R123, R141b, R245fa, and R600a refrigerants is shown in Tables 2, 3, and 4, for temperature, pressure, and enthalpy, respectively. These properties aided the computations of environmental impacts based on the methodology provided with respect to the system's power output as obtained in Lie et al., (2013).

Table 2: System operating temperatures

State point	Operating temperatures (K)					
	R113	R114	R123	R141b	R245fa	R600a
1	450	423	473	473	393	423
2	383	343	343	373	363	363
3	411.4	390.4	437.3	430.6	343.5	389.3
4	390.9	357.4	387.7	393.6	339.2	359.2
5	390.9	338	364.8	371.3	329.3	321.1
6	339.2	293	317.8	322.6	303.6	277.1
7	339.2	293	317.8	322.6	303.6	277.1
8	367.1	326.9	337.7	358.4	338.9	341.4
9	390.9	338	364.8	371.3	329.3	321.1
10	391.8	338.8	365.5	372.1	329.9	321.8
11	623	623	623	623	623	623
12	423	423	423	423	423	423
13	300	300	300	300	300	300
14	274	274	274	274	274	274
15	293	293	293	293	293	293
16	308	308	308	308	308	308
17	390.9	338	364.8	371.3	329.3	321.1

Table 3: System operating pressures

State point	Operating pressures (Bar)					
	R113	R114	R123	R141b	R245fa	R600a
1	18	18	18	18	18	18
2	2.35	0.9639	0.2237	1.207	7.991	2.635
3	6.5	6.5	6.5	6.5	4.129	6.5
4	6.5	6.5	6.5	6.5	4.129	6.5
5	6.5	6.5	6.5	6.5	4.129	6.5

6	1.8	1.8	1.8	1.8	1.8	1.8
7	1.8	1.8	1.8	1.8	1.8	1.8
8	3.784	4.915	3.252	4.806	5.434	10.45
9	6.5	6.5	6.5	6.5	4.129	6.5
10	18	18	18	18	18	18
11	1.013	1.013	1.013	1.013	1.013	1.013
12	1.013	1.013	1.013	1.013	1.013	1.013
13	1.013	1.013	1.013	1.013	1.013	1.013
14	1.013	1.013	1.013	1.013	1.013	1.013
15	1.013	1.013	1.013	1.013	1.013	1.013
16	1.013	1.013	1.013	1.013	1.013	1.013
17	6.5	6.5	6.5	6.5	4.129	6.5

Table 4: System operating enthalpies

State point	Operating enthalpies (KJ/Kg)					
	R113	R114	R123	R141b	R245fa	R600a
1	462.6	273.5	524.5	429.5	487.9	812.5
2	430.7	224	432	355	473.2	714.2
3	447.1	256.4	501.9	400.8	460.5	760.2
4	430.3	229	457.9	364.6	455.9	696.4
5	312.9	103	298.9	159.2	274.9	317.5
6	312.9	103	298.9	159.2	274.9	317.5
7	399.5	185.9	410	311.1	426.8	560.4
8	416.6	206.7	422	335.1	452.1	644.3
9	312.9	103	298.9	159.2	274.9	317.5
10	313.8	103.9	299.8	160.2	276	319.7
11	631.6	631.6	631.6	631.6	631.5	631.6
12	424.6	424.6	424.6	424.6	424.6	424.6
13	300.4	300.4	300.4	300.4	300.4	300.4
14	274.3	274.3	274.3	274.3	274.3	274.3
15	83.38	83.38	83.38	83.38	83.3	83.38
16	146.1	146.1	146.1	146.1	146	146.1
17	312.9	103	298.9	159.2	274.9	317.5

4.1 Results from emissions

The results of the GHG emissions profile of the power-cooling cycle is shown for R113, R114, R123, R141b, R245fa, and R600a. The system was modelled with a yearly operation time of 7,000 hours and a lifetime of 20 years. These parameters, along with the environmental emissions inventory of the system in operation phase were used to model the emissions profile of the system. The system was simulated with the same inlet heat source parameters for each refrigerant; however, the turbine inlet temperature (TIT) and pressure (TIP) were varied based on the thermal properties of each refrigerant. The turbine output power for each refrigerant under these conditions is shown in Table 5.

Table 5: Turbine Output Power for each Refrigerant at Turbine Inlet of 450 K and 18 Bar

Refrigerant	Turbine output power (kW)		Turbine output power (kWh)
R113	65.95		0.018319444
R114	123		0.034166667
R123	121		0.033611111
R141b	107.8		0.029944444
R245fa	155.1		0.043083333
R600a	297.5		0.082638889

4.2 Evaluation of the GHG emissions profile of the plant

The environmental impact from each refrigerant is presented with respect to the quantity of respective harmful gasses per power of turbine output in the cycle. In the operation phase of the plant, the indicators are presented in Table 6 for all considered refrigerants.

Table 6: Environmental emissions inventory of the power-cooling cycle in operation phase (Liu et al., 2013)

Refrigerants	Emissions factor (kg/kWh)			
	CO ₂ ($\times 10^{-2}$)	CH ₄ ($\times 10^{-5}$)	NO _x ($\times 10^{-4}$)	CO ($\times 10^{-5}$)
R113	1.11	3.36	0.804	1.59
R114	5.20	15.7	3.76	7.42
R123	1.71	5.17	1.24	2.44
R141b	1.50	4.52	1.08	2.13
R245fa	3.43	10.4	2.48	4.89
R600a	1.81	5.47	1.31	2.58

Corresponding to the turbine output power obtained (Table 7) and the environmental emission inventory in Table 6, the GHG emissions pattern is shown in Fig. 2 for throughout the 20-year life cycle. Based on the power output from the system, and the GWP of the refrigerants, the emissions profile varies accordingly. Carbon dioxide is the predominant GHG followed by sulphur dioxide and nitrogen oxide. The refrigerant R114 possess the highest environmental impact, as well as R600a. R113 possessed the least environmental impact when used as the working fluid. However, the highest power output from the system results from the utilization of R600a, but with very high environmental impact.

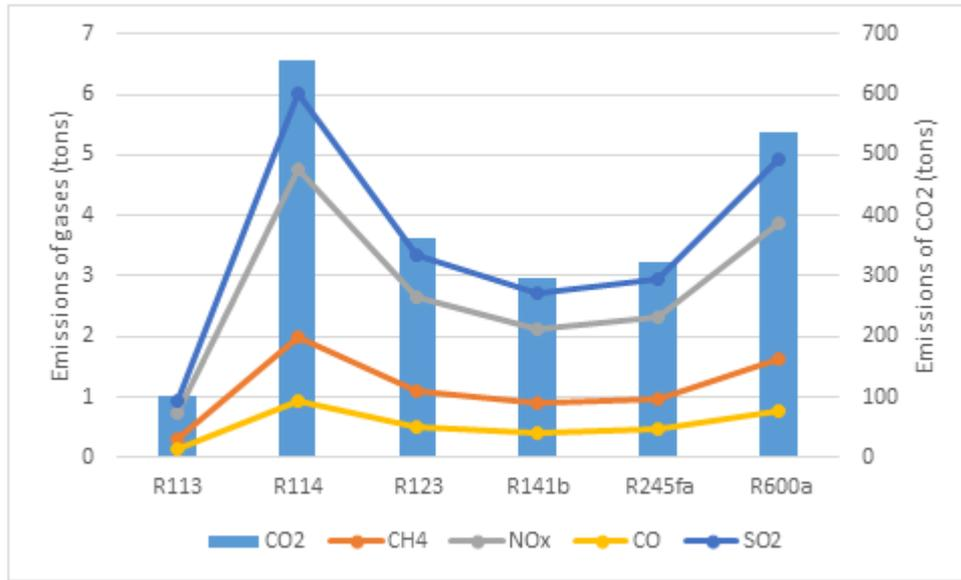


Fig. 2: Lifetime emissions of power-cooling cycle for different refrigerants at turbine inlet of 450 K and 18 Bar

Across all the refrigerants, the results show that CO₂ is the gas that is produced/evolved the most, with it being evolved at least 108.8 times more than the next gas (SO₂). Following down the line is NO_x, before CH₄ (methane) and lastly CO (carbon monoxide). Most amount of emissions is produced by the refrigerants in the order: R114, R600a, R245fa, R123, R141b and R113. These results hold true when all refrigerants operate at the same turbine inlet temperature (TIT) and turbine inlet pressure of 450 K and 18 bar respectively. Furthermore, at the same pressure of 18 bar, the TIT is altered to suit each refrigerant based on their thermodynamic properties, and the resulting output power in *Table 7* and the emissions from each refrigerant in *Fig. 3*. The emissions pattern in *Fig. 3* has a direct bearing with same operating conditions in *Fig. 2*.

Table 7: Turbine Output Power for each refrigerant at optimized turbine inlet temperatures

Refrigerant	Turbine Inlet Temperature (K)	Turbine output power (kW)	Turbine output power (kWh)
R113	450	65.95	0.018319444
R114	423	90.39	0.025108333
R123	473	151.9	0.042194444
R141b	473	141	0.039166667
R245fa	393	66.98	0.018605556
R600a	423	212	0.058888889

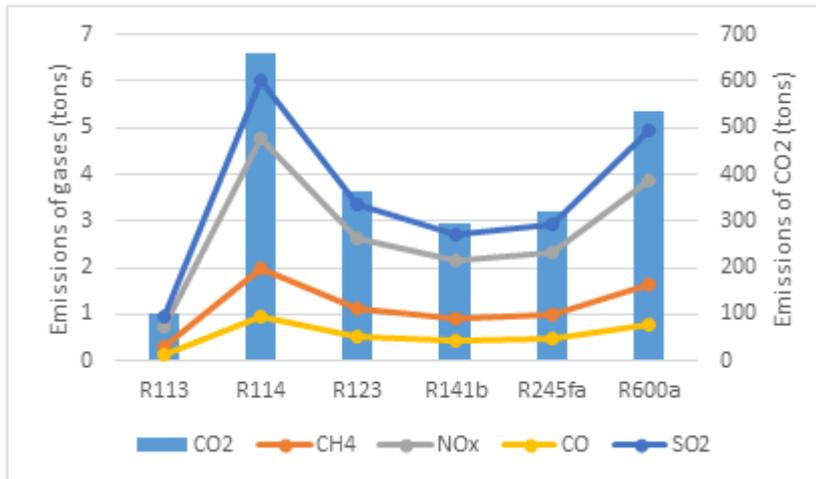


Fig. 3: Lifetime emissions of power-cooling system for different refrigerants at optimized turbine inlet temperatures

With the adjustment to the TIT, R245fa produced 56.8% less emissions. Conversely, R123 and R141b produced 25.5% and 30.8% more emissions respectively; the two highest increases.

4.3 Comparative evaluation of the system's thermodynamic performance and emissions generated with different refrigerants

For a better expression of the effects of each gas emitted, it is necessary to effectively express the emissions of the various gases as one common parameter referred to as the CO₂ equivalent of the gases. The CO₂ equivalent for each gas represents the number of units of CO₂ gas that would be equal to one unit of the evolved gas. It is obtained by multiplying the amount of gas evolved by the global warming potential (GWP) of that gas. Because the CO₂ equivalent is measured in units of CO₂ gas, the GWP of CO₂ is 1. The GWP is only expressed for gases that are considered as greenhouse gases. For this reason, SO₂ is excluded from this conversion since it is not a greenhouse gas.

Considering the lifetime of the power-cooling cycle, the emissions produced by the system for each refrigerant based on the output power produced by the turbine is presented in Fig. 4. The power-cooling cycle will pose less environmental impact when R113 is used as the working fluid but with a 27 % reduction in estimated net turbine output compared to R114.

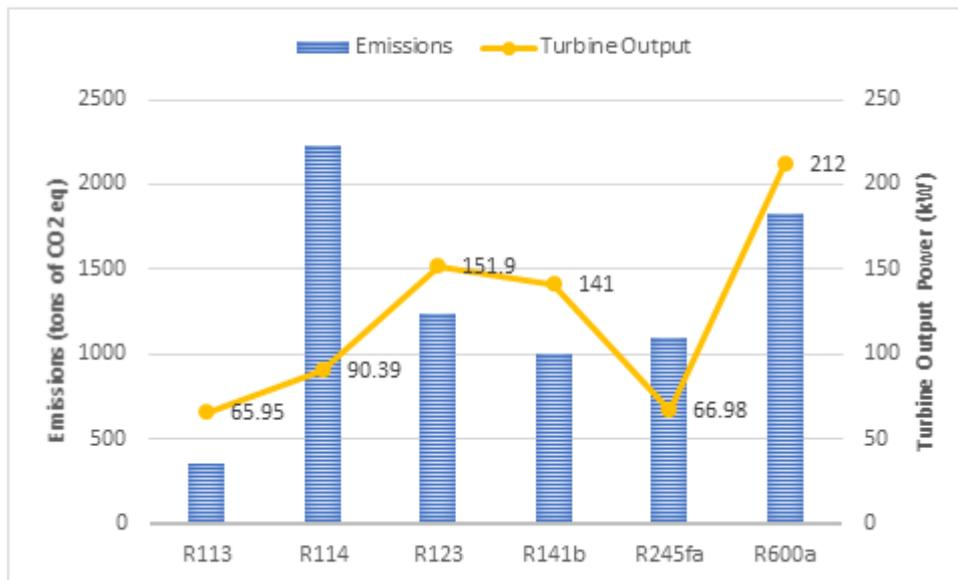


Fig. 4: Lifetime CO₂-eq emissions of power-cooling cycle by output power

4.4 Sensitivity analysis of the operating parameters on the performance of the system

Sensitivity analysis was performed on the power-cooling cycle system to evaluate variables that considerably influence the system's performance.

i. Effect of turbine inlet temperature on emissions (CO₂ eq) produced

To carry out a test on the effect of variations in turbine inlet temperature on the emissions produced, the turbine inlet pressure for the power-cooling cycle was kept constant at 18 Bar. The results of the variation of turbine inlet temperature (TIT) on the emissions produced is shown in Fig. 5.

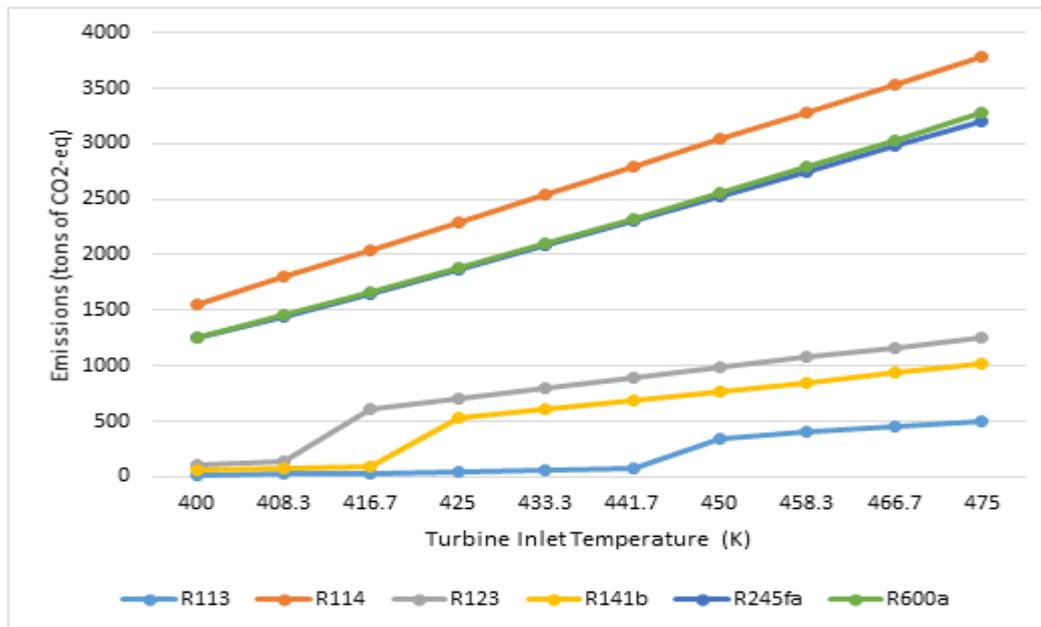


Fig. 5: Effect of turbine inlet temperature on emissions produced

Across the board, the emissions produced increases with an increase in the turbine inlet temperature. Within the range that was worked with (i.e., 400 K to 475 K), the highest amount of emissions produced by each refrigerant was obtained at 475 K but the trend signifies that the increase in emissions will indefinitely get higher as long as the temperature is increased; perhaps until it the refrigerant no longer becomes useable in the power-cooling cycle at a particular temperature (which was not attained in this particular sensitivity analysis).

In the graph for some refrigerants, we see “spikes” in the amount of emissions produced by the system. These spikes occur due to a change of state of the refrigerant from a subcooled liquid to a superheated gas. As the refrigerants change their state, they get more energy to drive the turbine in order to produce a greater output power from the turbine. The amount of power produced by the turbine is directly proportional to the emissions evolved, thus, this increase.

The result of this analysis infers that along an isobaric line (considering a refrigerant in its superheated gas phase), the output from the turbine, and thus the emissions produced by the system, would be the lowest possible at the temperature where the working fluid is just superheated.

ii. Effect of turbine inlet pressure on turbine output power (kW) and emissions produced (CO₂ eq)

To obtain the effect that a change in turbine inlet pressure would have on the emissions produced from the power-cooling cycle, the turbine inlet temperature of the system is kept constant at 450 K while the pressure is varied between 13 bar and 23 bar. The results of the variation of turbine inlet pressure on the emissions produced is shown in Table 8.

We immediately note that pressure variation at constant temperature does not cause as great a change in emissions produced as like temperature variation at constant pressure. The trend across all refrigerants is not uniform at every point, but it can be deciphered that the effect of pressure increase at constant temperature on the amount of power, and thus the emissions, produced is

subject to the law of diminishing effectas the power produced increases at a diminishing rate with equal increases in turbine inlet pressure. In some cases, (i.e., for R113, R114, R123, and R141b) the power produced is seen to flat-line, or begin decreasing, within the pressure range that the sensitivity analysis was conducted.

Table 8: Effect of turbine inlet pressure on turbine output power and emissions produced

Turbine Pressure (bar)	Turbine Output Power (kW) Emissions Produced (CO2 eq)											
	R113		R114		R123		R141b		R245fa		R600a	
13	66.91	353.15	117.6	2904.14	117.1	952.84	102.6	728.72	148.4	2417.45	276.6	2379.17
14.11	67.37	355.58	119.2	2943.65	118.5	964.23	104.4	741.51	150.4	2450.03	282.5	2429.92
15.22	67.45	356	120.6	2978.23	119.6	973.18	105.9	752.16	152.1	2477.72	287.6	2473.78
16.33	67.16	354.47	121.7	3005.39	120.4	979.69	106.9	759.26	153.5	2500.53	292	2511.63
17.44	66.46	350.77	122.6	3027.62	120.9	983.76	107.6	764.24	154.7	2520.08	295.8	2544.32
18.56	65.32	344.76	123.3	3044.9	121.1	985.39	107.9	766.37	155.5	2533.11	299.1	2572.7
19.67	18.5	97.64	123.8	3057.25	121	984.57	107.9	766.37	156.2	2544.51	301.8	2595.93
20.78	18.7	98.7	124.2	3067.13	120.8	982.95	107.6	764.24	156.7	2552.66	304.2	2616.57
21.89	18.9	99.75	124.4	3072.07	120.2	978.07	106.9	759.26	156.9	2555.92	306.2	2633.77
23	19.1	100.81	124.4	3072.07	119.4	971.56	105.9	752.16	157	2557.54	307.8	2647.53

For R113, we see the diminishing effect occur early on after 15.22 bar before a drastic drop in output power, but this significant drop happens as a result of a change in state of R113 from a superheated gas to a subcooled liquid.

The result of this sensitivity analysis indicates that pressure is not an operating parameter that can be invariably increased in order to obtain an increase in power output, but rather, an optimal pressure for the operation of the system at a particular temperature should be obtained and used. A further result of the analysis signifies that along an isotherm, the optimal pressure that would produce the highest power output from the turbine would be the pressure value at the point where the working fluid just becomes superheated.

5.0 Conclusion

The GHG emissions potential of an adapted power-cooling cycle was analyzed using for R113, R114, R123, R141b, R245fa, and R600a. The focus was on the operation phase of the plant which is known to contribute more to GHG emissions than the manufacturing and decommissioning phases in the system's life cycle. The following major conclusions are made:

- With similar turbine inlet operating pressure and temperature of 18 Bar and 450 K, respectively, the refrigerants decreasing emissions profile were the order: R114, R600a, R245fa, R123, R141b and R113.
- Carbon dioxide had the higher emission potential in the system for all considered refrigerants, about 108.8 times than SO₂, NO_x, and CH₄.
- The power-cooling cycle will pose less environmental impact when R113 is used as the working fluid but with a 27 % reduction in estimated net turbine output compared to R114.
- The emissions produced increases with an increase in the turbine inlet temperature.

References

1. Abam, F. I., Okon, B. B., B Ekwe, E., Isaac, J., O Effiom, S., C Ndukwu, M., Inah, O. I., A Ubi, P., Oyedepo, S., & S Ohunakin, O. (2022). Thermoeconomic and exergoenvironmental sustainability of a power-cooling organic Rankine cycle with ejector system. *E-Prime - Advances in Electrical Engineering, Electronics and Energy*, 2, 100064.
2. Ayub, M., A. Mitsos, and H. Ghasemi, Thermo-economic analysis of a hybrid solar-binary geothermal power plant. *Energy*, 2015. 87: p. 326-335.
3. Bian, Q. (2020). Waste heat: the dominating root cause of current global warming. *Environmental Systems Research* 2020 9:1, 9(1), 1–11.
4. Bronicki, L. (2017). History of Organic Rankine Cycle systems. In *Organic Rankine Cycle (ORC) Power Systems: Technologies and Applications* (pp. 25–66).
5. Cao, L., Wang, J., Wang, H., Zhao, P., & Dai, Y. (2017). Thermodynamic analysis of a Kalina-based combined cooling and power cycle driven by low-grade heat source. *Applied Thermal Engineering*, 111, 8–19.
6. Guzović, Z., P. Rašković, and Z. Blatarić, The comparison of a basic and a dual-pressure ORC (Organic Rankine Cycle): Geothermal Power Plant Velika Ciglena case study. *Energy*, 2014. 76: p. 175-186.
7. Haghparast, P., Sorin, M. V, Richard, M. A., & Nesreddine, H. (2019). Analysis and design optimization of an ejector integrated into an organic Rankine cycle. *Applied Thermal Engineering*, 159, 113979.
8. Li, H., Yang, S., & Qian, Y. (2012). Life cycle assessment of coal-based methanol. *Computer Aided Chemical Engineering*, 31, 530–534.
9. Liu, C., He, C., Gao, H., Xie, H., Li, Y., Wu, S., & Xu, J. (2013). The environmental impact of organic Rankine cycle for waste heat recovery through life-cycle assessment. *Energy*, 56, 144–154.
10. Manente, G., Lazzaretto, A., & Bonamico, E. (2017). Design guidelines for the choice between single and dual pressure layouts in organic Rankine cycle (ORC) systems. *Energy*, 123, 413–431.
11. Mohammadzadeh Bina, S., Jalilinasrabady, S., & Fujii, H. (2017). Energy, economic and environmental (3E) aspects of internal heat exchanger for ORC geothermal power plants. *Energy*, 140, 1096–1106.
12. Mondal, S., & De, S. (2017). Ejector based organic flash combined power and refrigeration cycle (EBOFCP&RC) – A scheme for low grade waste heat recovery. *Energy*, 134, 638–648.
13. Mondejar, M. E., Andreasen, J. G., Pierobon, L., Larsen, U., Thern, M., & Haglind, F. (2018). A review of the use of organic Rankine cycle power systems for maritime applications. *Renewable and Sustainable Energy Reviews*, 91, 126–151.
14. Park, J., Jung, I., Choi, W., Choi, S. O., & Han, S. W. (2019). Greenhouse gas emission offsetting by refrigerant recovery from WEEE: A case study on a WEEE recycling plant in Korea. *Resources, Conservation and Recycling*, 142, 167–176.
15. Wang, S., Liu, C., Ren, J., Liu, L., Li, Q., & Huo, E. (2019). Carbon footprint analysis of organic Rankine cycle system using zeotropic mixtures considering leak of fluid. *Journal of Cleaner Production*, 118095.
16. Yu, G., et al., Simulation and thermodynamic analysis of a bottoming Organic Rankine Cycle (ORC) of diesel engine (DE). *Energy*, 2013. 51: p. 281-290.